Supporting Information for

Hyaluronic Acid Hydrogels with Phototunable Supramolecular Crosslinking for Spatially Controlled Lymphatic Tube Formation

Fei Fan,[†] Bo Su,[§] Alexander Kolodychak,[§] Ephraim Ekwueme,[†] Laura Alderfer,[†] Sanjoy Saha,[†] Matthew J. Webber,[§] and Donny Hanjaya-Putra*[†]*

[†] Bioengineering Graduate Program, Aerospace and Mechanical Engineering, University of Notre Dame, Notre Dame, IN 46556, USA

[§] Chemical and Biomolecular Engineering, University of Notre Dame, Notre Dame, IN 46556, USA.

This supplementary information includes:

Supplementary Figure S1 to S31
Scheme S1 to S2

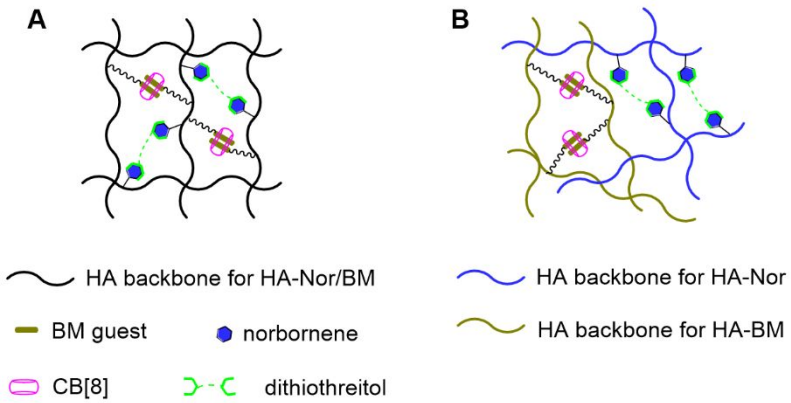

Figure S1. Schematic illustration of (A) dual-crosslinked HA-Nor/BM/CB[8] hydrogel and (B) double-network HA-Nor&HA-BM/CB[8] hydrogel. For clarity, the HA polymers modified with both Nor and BM are shown in black, HA polymers modified with Nor and BM separately are shown in different colors (blue and olive).

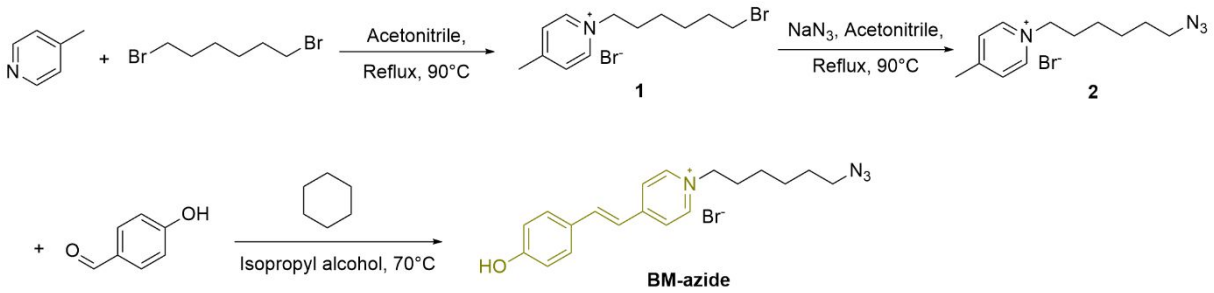

Scheme S1. Synthesis of BM-azide.

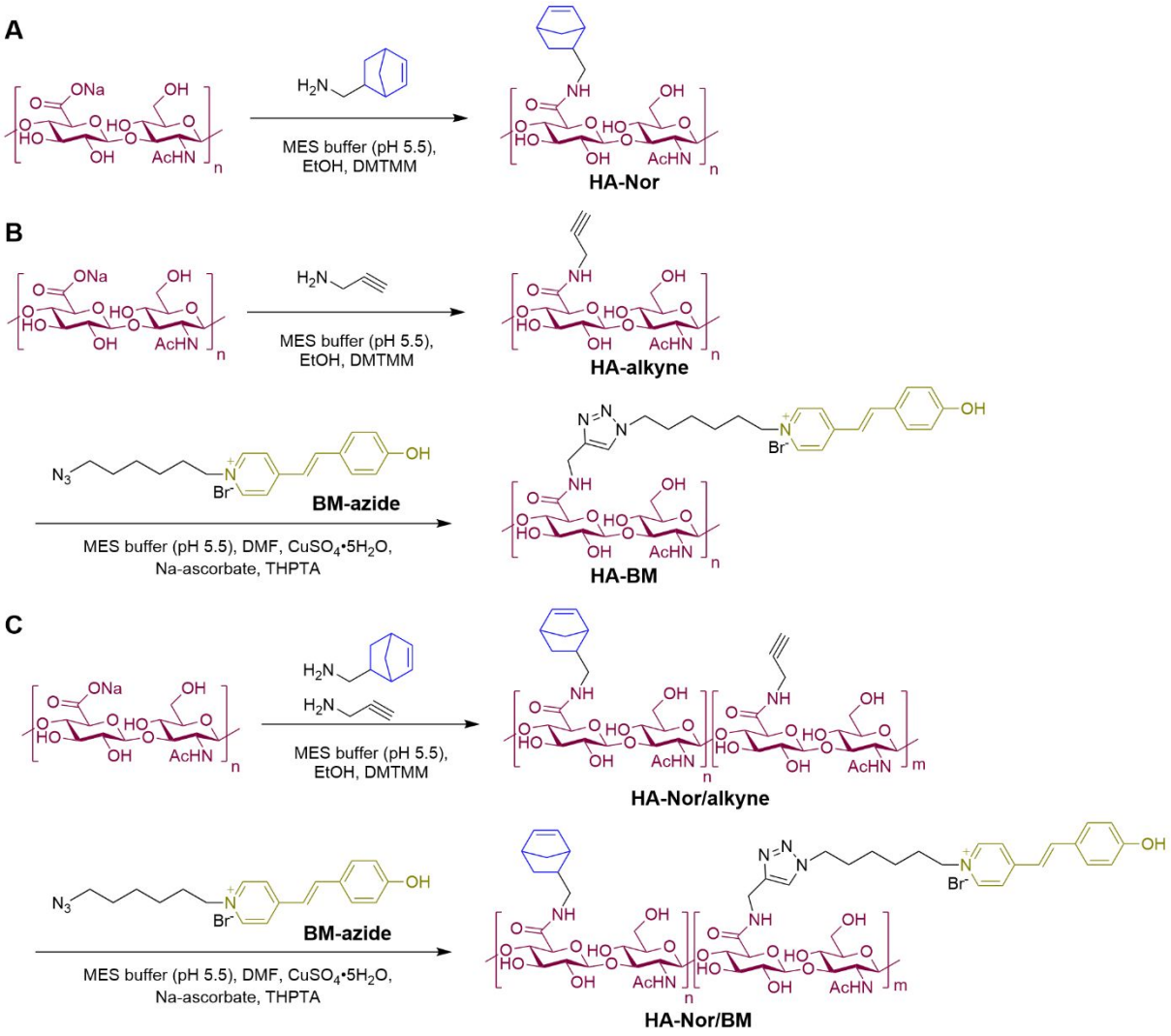

Scheme S2. Synthesis of (A) HA-Nor, (B) HA-BM and (C) HA-Nor/BM through DMTMM activated amidation and copper-catalyzed azide-alkyne cycloaddition.

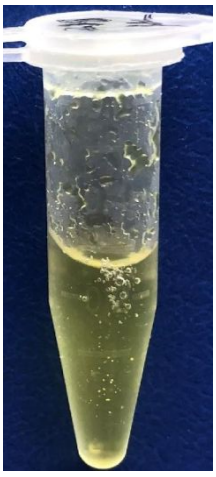

Figure S2. Representative picture of lyophilized HA-BM or HA-Nor/BM with high degree of substitution (DS) values were reconstituted in DI H_2O at 5 mg mL^{-1}. The polymers were dispersed in DI H_2O in the form of small hydrogels.

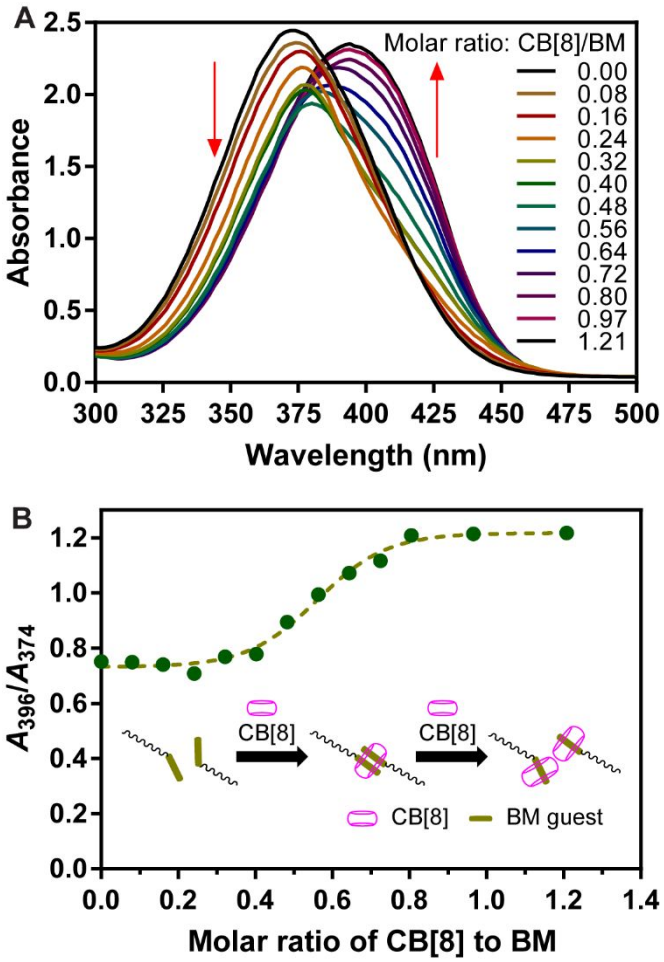

Figure S3. Supramolecular Interaction of HA-BM with CB[8] at 0.5 mg mL^{-1} HA-BM (192 μM BM). (A) Absorbance spectra of HA-BM in the presence of various molar ratios of CB[8]. The maximum absorbance wavelength was shifted from 374 nm to 396 nm and the ratios of absorbance at 396 nm to 374 nm increased (B) with an increase in CB[8] molar ratio.

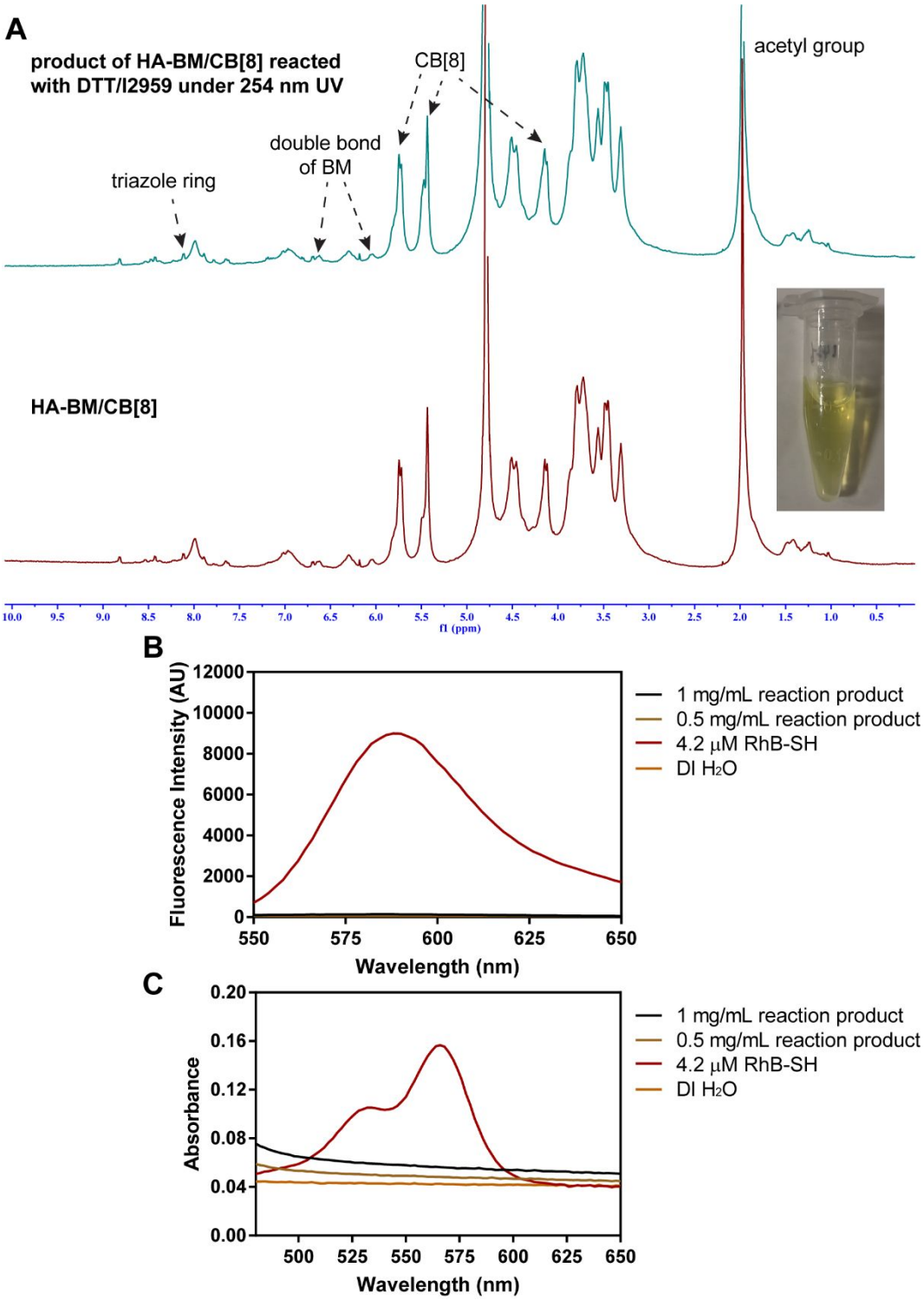

Figure S4. HA-BM/CB[8] complex can not react with thiol containing molecules. (A) ^{1}H NMR of HA-BM/CB[8] before and after reacted with DTT/I2959 under 254 nm UV irradiation, the insert picture showed reaction mixture was clear without gelation or precipitation. (B) Emission spectrum (excitation wavelength 520 nm) and (C) absorbance spectrum of HA-BM/CB[8] after reacting with RhB-SH/I2959 under 254 nm UV irradiation.

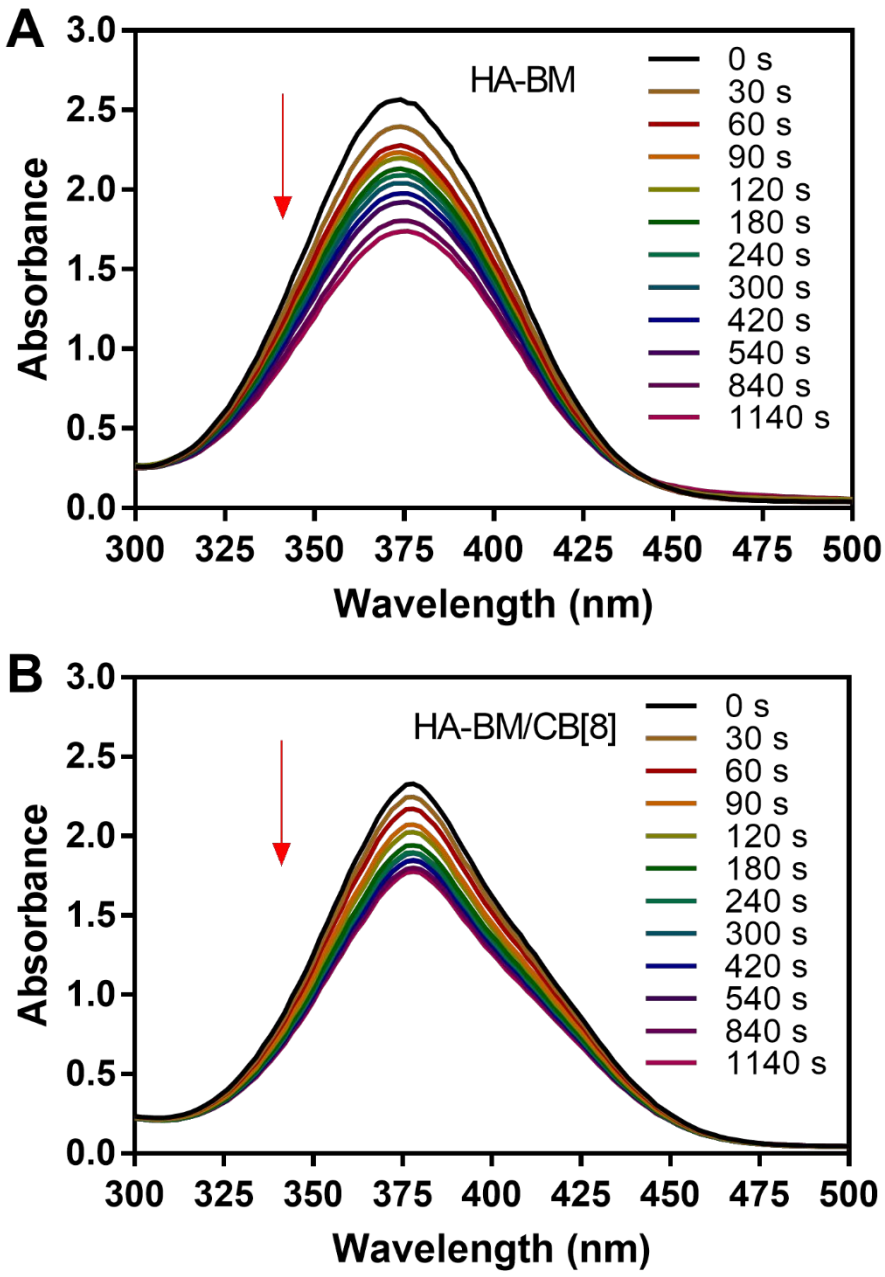

Figure S5. Absorbance spectra of 0.5 mg mL^{-1} HA-BM (192 μM BM) with 254 nm UV light irradiation over time in the (A) absence or (B) presence of CB[8].

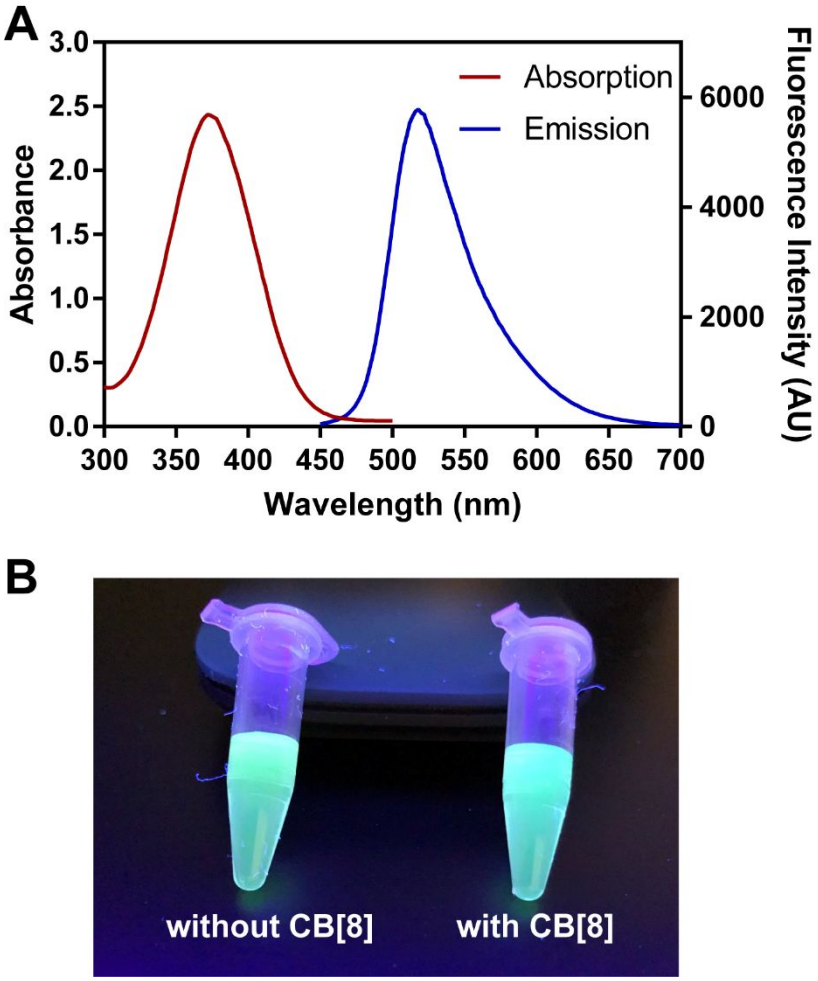

Figure S6. Fluorescence property of HA-BM: (A) absorption and emission scanning spectra (excitation wavelength 378 nm) of 0.5 mg mL^{-1} HA-BM (192 μM BM), (B) HA-BM solution with or without CB[8] upon a UV lamp (365 nm) exposure.

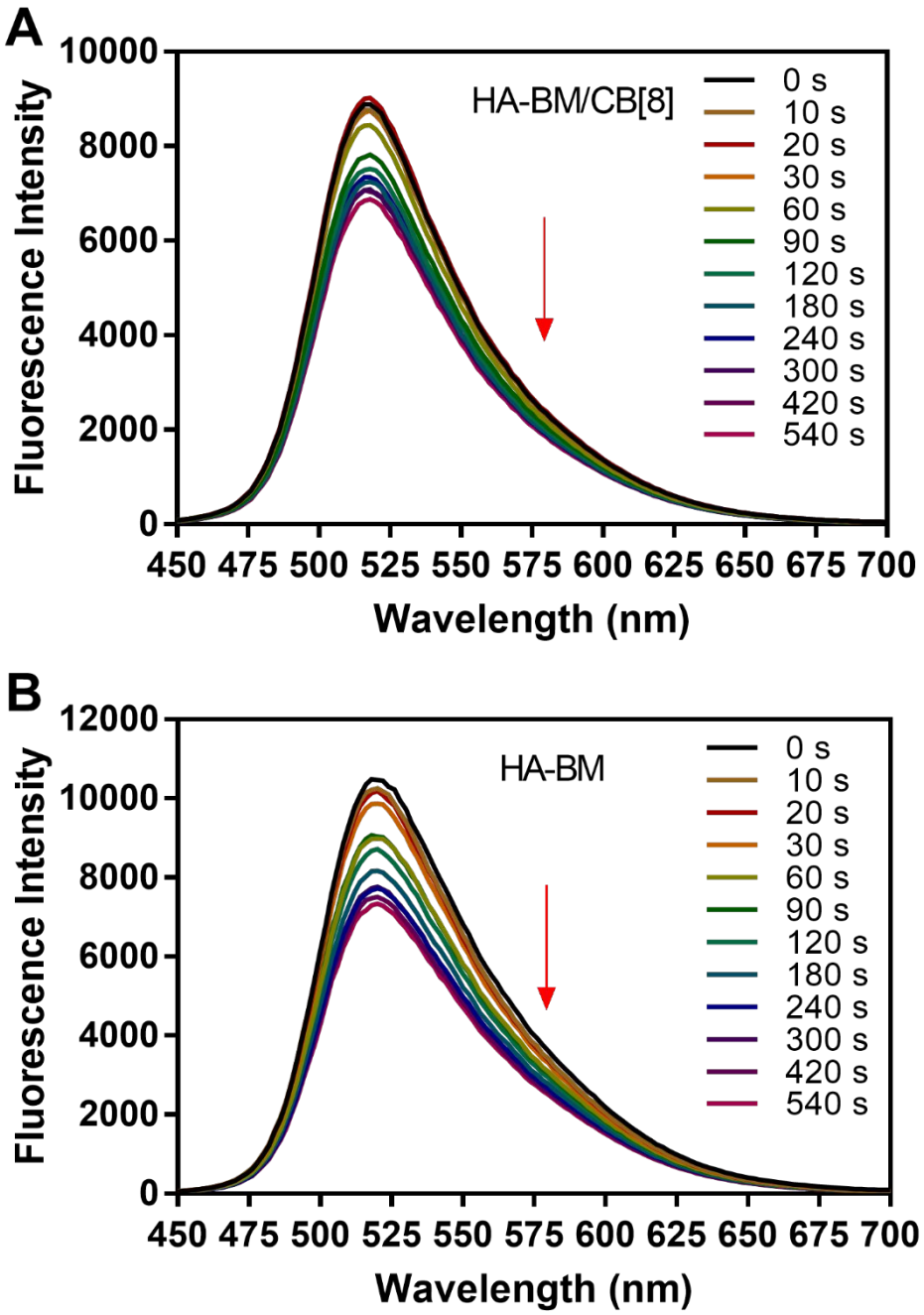

Figure S7. Fluorescence spectra (excitation wavelength 378 nm) of 0.5 mg mL^{-1} HA-BM (192 μM BM) with 365 nm UV light irradiation over time in the (A) presence or (B) absence of CB[8].

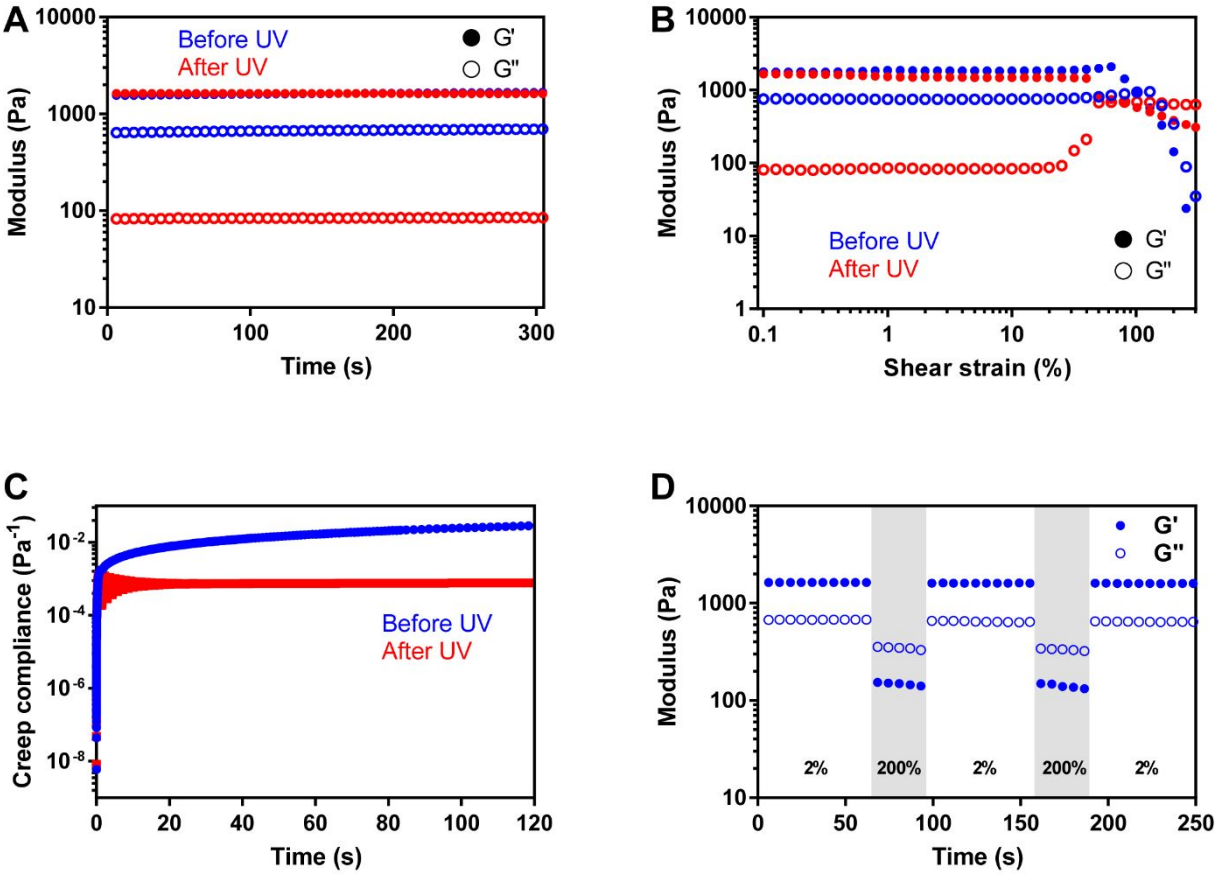

Figure S8. Rheology tests for HA-BM/CB[8] hydrogel. (A) Time sweep (2% strain, 10 rad s^{-1}), (B) strain sweep (10 rad s^{-1}), (C) creep (100 Pa stress) rheology of HA-BM/CB[8] hydrogel before UV (blue), after 365 nm UV (red) irradiation. (D) Step strain rheology of HA-BM/CB[8] hydrogel before UV irradiation under cyclic 2% and 200% (gray shaded) strain loading.

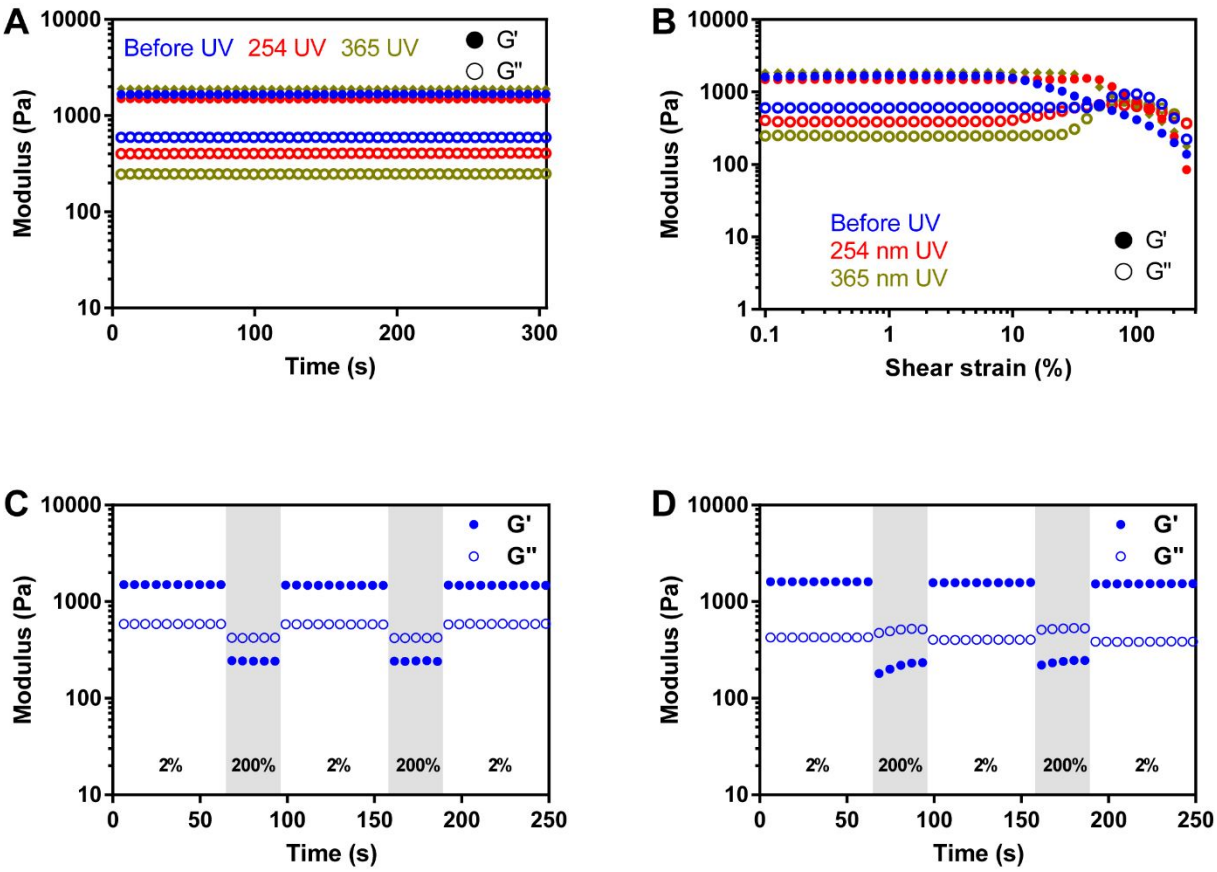

Figure S9. Rheology tests for dual-crosslinked HA-Nor/BM/CB[8] hydrogel. (A) Time sweep (2% strain, 10 rad s^{-1}), (B) strain sweep (10 rad s^{-1}) rheology of HA-Nor/BM/CB[8] hydrogel before UV (blue), after 254 nm UV (red) and 365 nm UV (olive) irradiation. Step strain rheology of HA-Nor/BM/CB[8] hydrogel (C) before UV and (D) after 254 nm UV irradiation under cyclic 2% and 200% (gray shaded) strain loading.

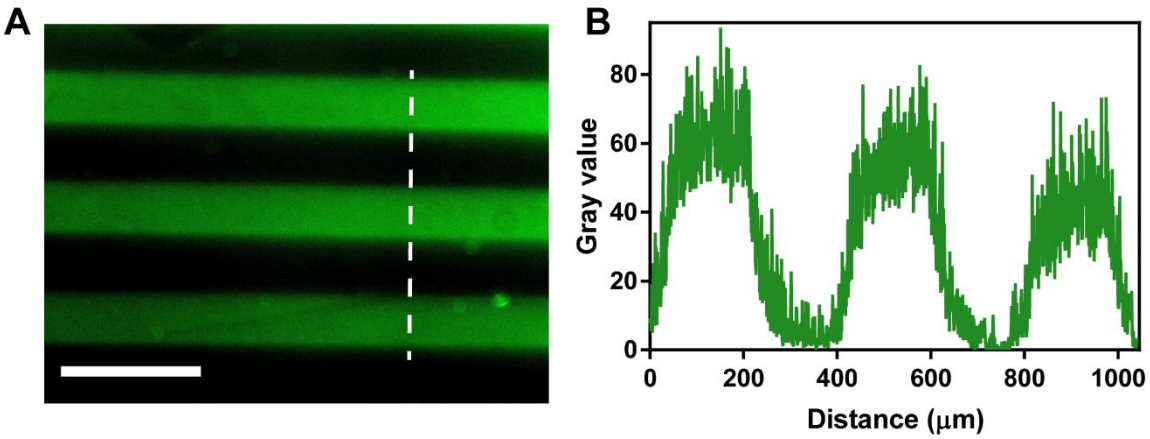

Figure S10. Photopatterning of HA-Nor/DTT hydrogel with FL-peptide dye with 200 μm stripes mask. (A) The patterns were imaged by FTIC (green) filters of microscopy. Scale bar: 500 μm. (B) Fluorescence intensity profile of green color was quantified along the dashed white line.

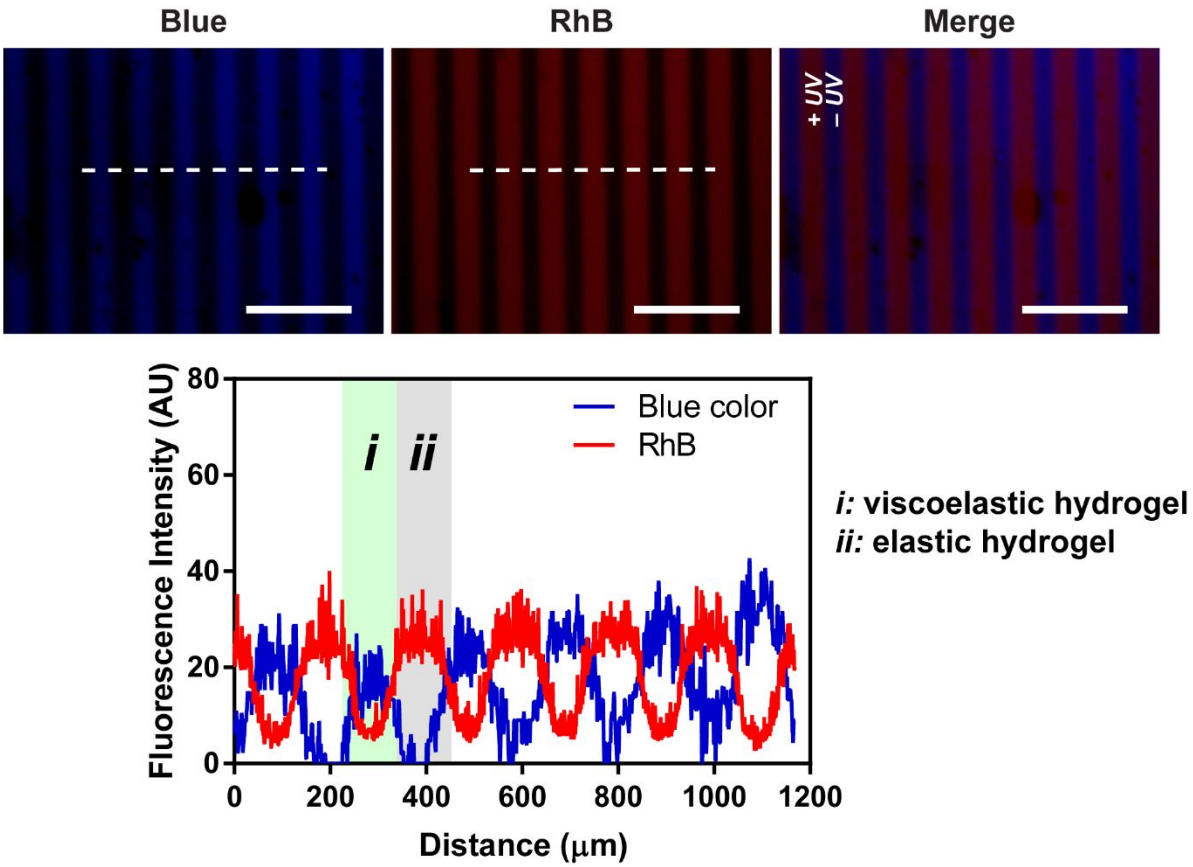

Figure S11. Photopatterning of dual-crosslinked HA-Nor/BM/CB[8] hydrogel with 100 μm stripes mask. The patterns were imaged by DAPI (blue) and Texas Red (red) filters of microscopy, with fluorescence intensities were quantified along the dashed white line. *i*: viscoelastic hydrogel; *ii*: elastic hydrogel. Scale bar: 500 μm.

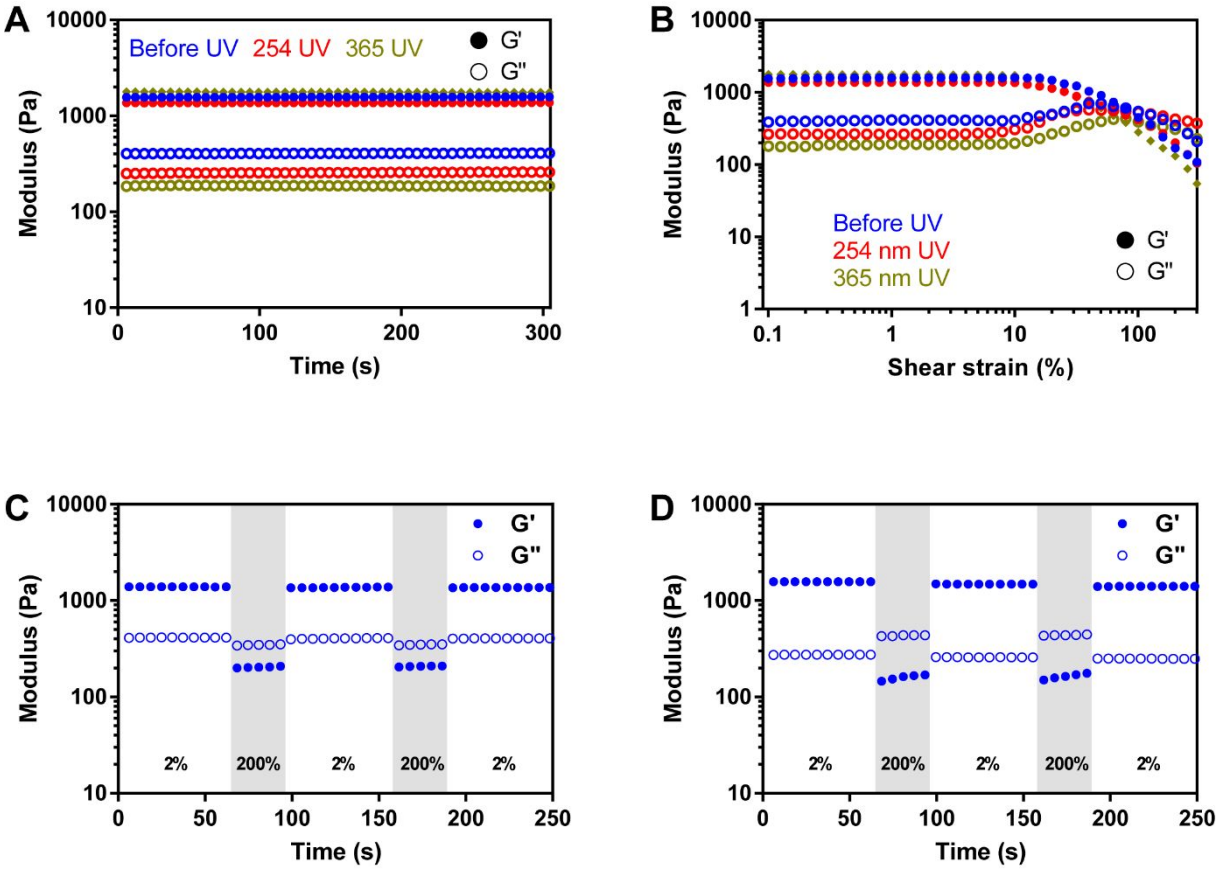

Figure S12. Rheology tests for double-network HA-Nor&HA-BM/CB[8] hydrogel. (A) Time sweep (2% strain, 10 rad s^{-1}), (B) strain sweep (10 rad s^{-1}) rheology of HA-Nor/HA-BM/CB[8] hydrogel before UV (blue), after 254 nm UV (red) and 365 nm UV (olive) irradiation. Step strain rheology of HA-Nor/HA-BM/CB[8] hydrogel (C) before UV and (D) after 254 nm UV irradiation under cyclic 2% and 200% (gray shaded) strain loading.

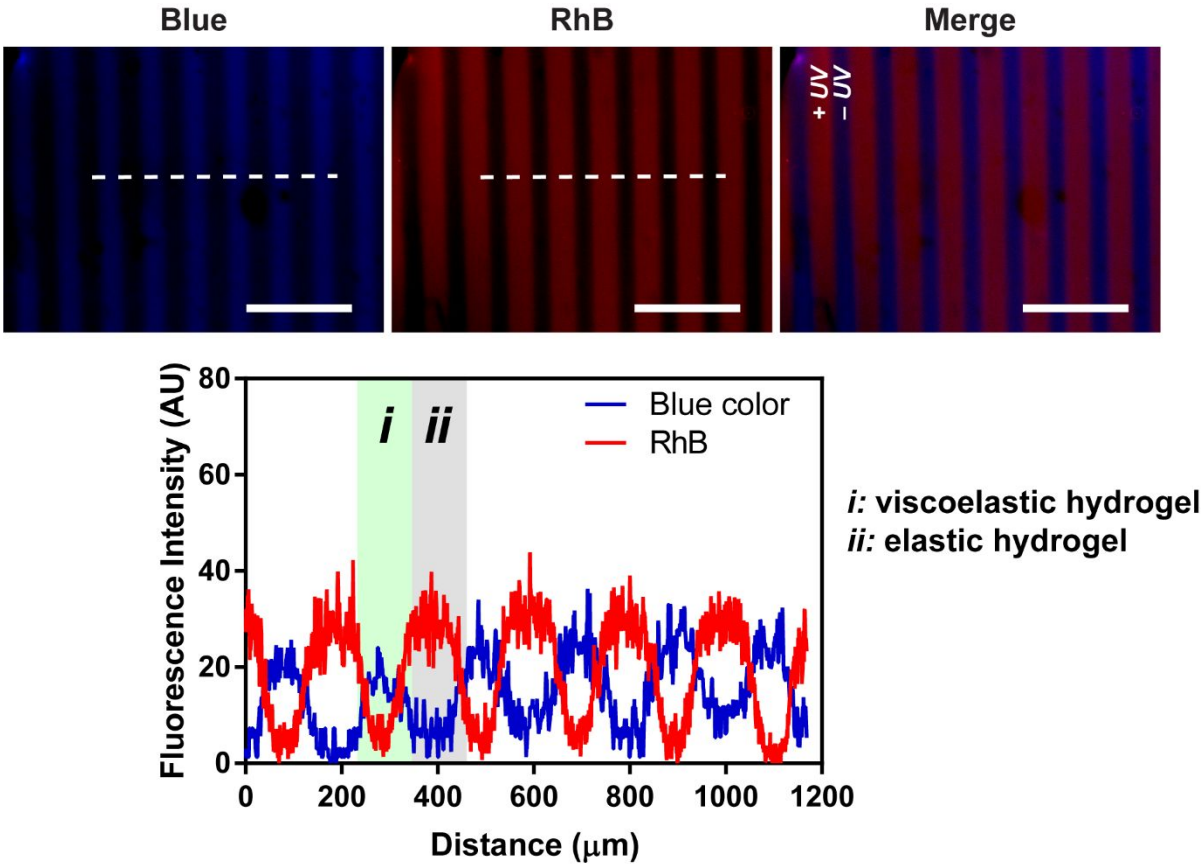

Figure S13. Photopatterning of double-network HA-Nor&HA-BM/CB[8] hydrogel with 100 μm stripes mask. The patterns were imaged by DAPI (blue) and Texas Red (red) filters of microscopy, with fluorescence intensities were quantified along the dashed white line. *i*: viscoelastic hydrogel; *ii*: elastic hydrogel. Scale bar: 500 μm.

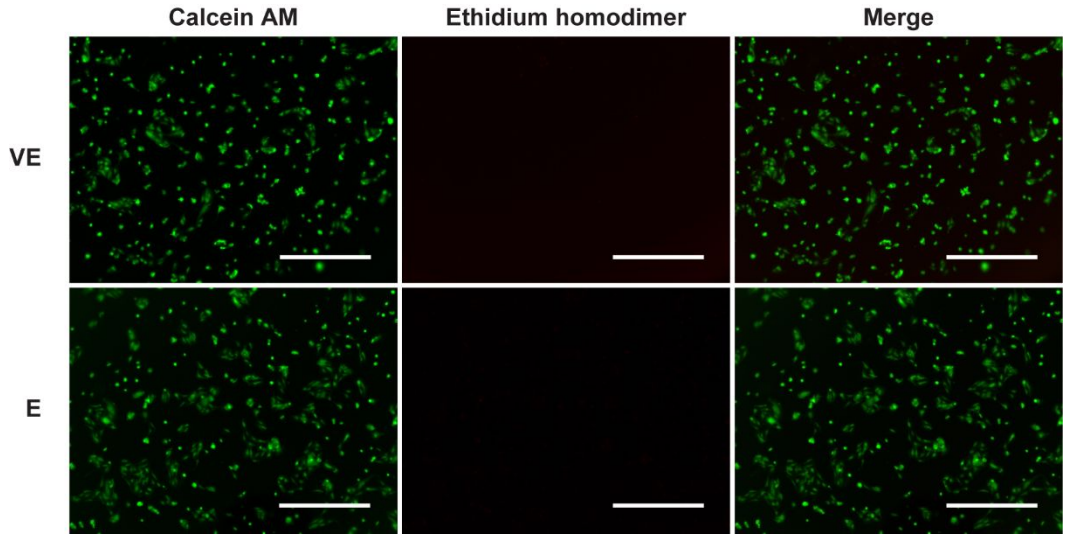

Figure S14. Cell viability of lymphatic endothelial cells (LECs) at day 3 on HA-Nor/BM/CB[8] hydrogels. Viscoelastic (VE) and elastic (E) hydrogels were prepared by 254 nm and 365 nm

UV light irradiation, respectively. LECs were stained with calcein AM (green) for live cells and ethidium homodimer-1 (red) for death cells. Scale bars: 500 μm.

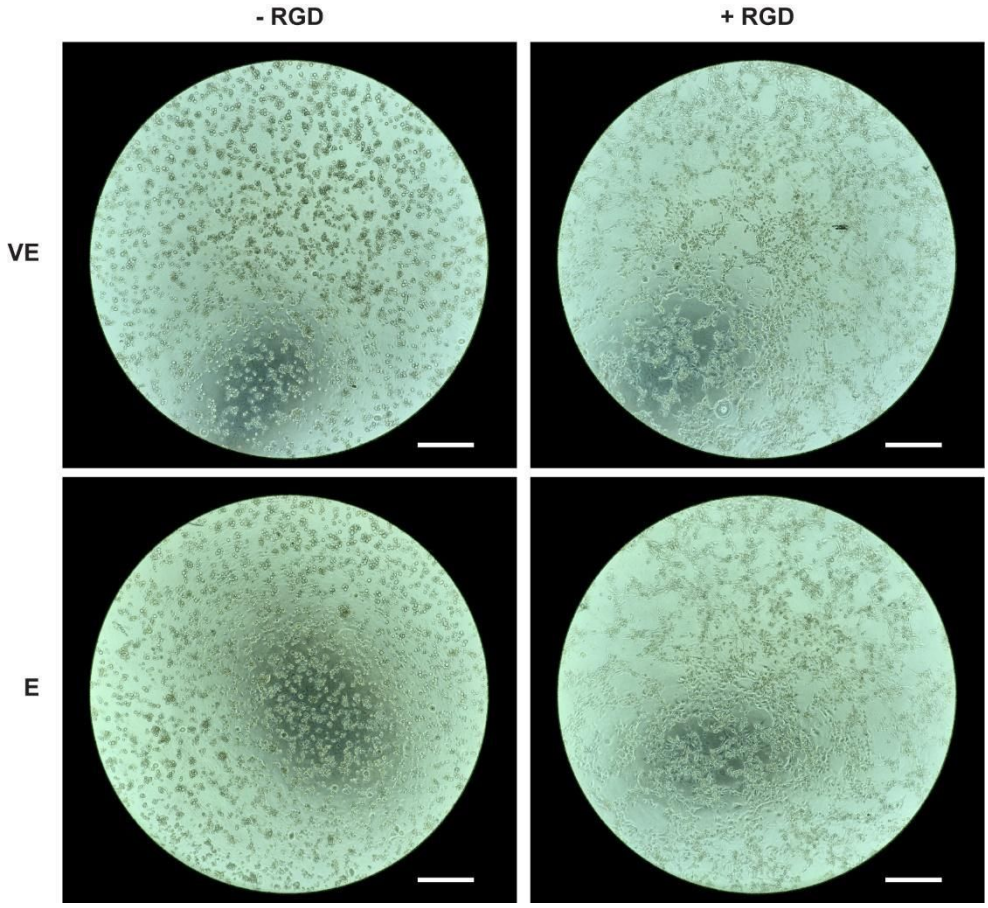

Figure S15. RGD peptide modification of hydrogel is indispensable for LECs attachment. LECs on viscoelastic (VE) and elastic (E) HA-Nor/BM/CB[8] hydrogels with RGD peptides showed stretched morphology, whereas LECs on the hydrogels without RGD peptides were round due to poor adhesion. Scale bars: 500 μm.

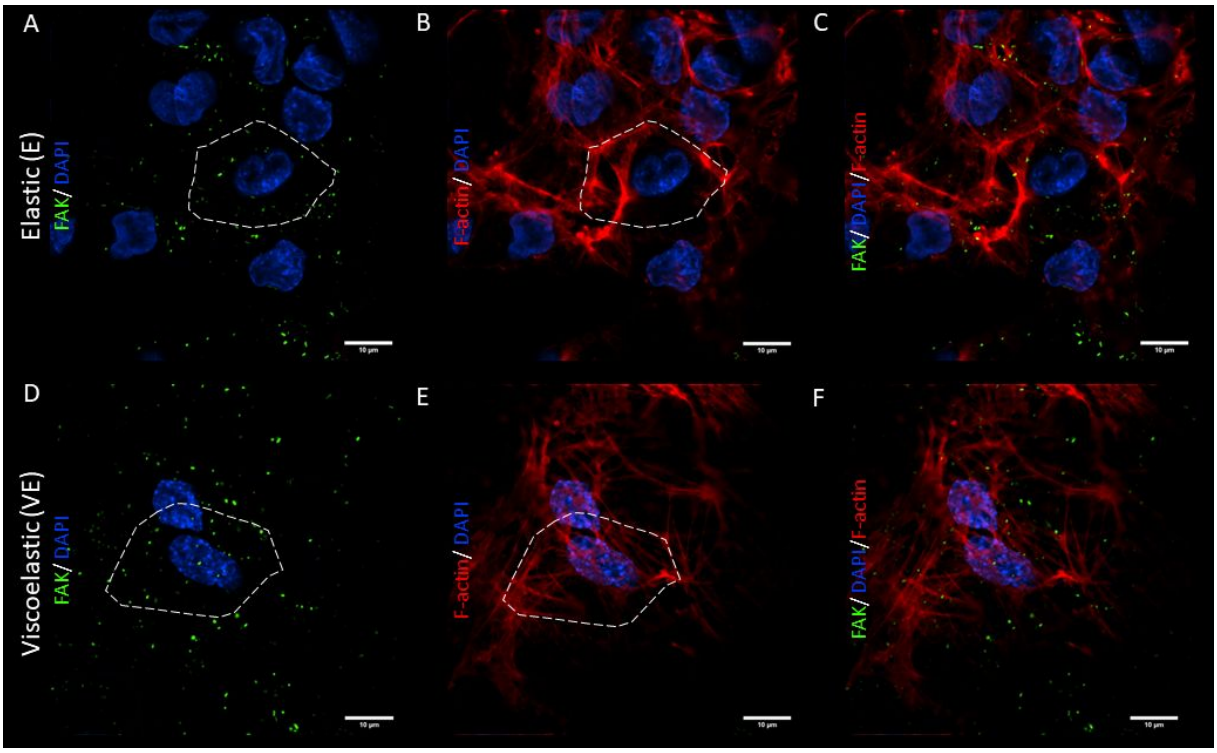

Figure S16. Focal adhesion kinase (FAK) and F-actin expression of LECs cultured on viscoelastic and elastic hydrogels. Representative immunofluorescent images of LECs cultured on hydrogels stained for FAK (green), F-actin (red), and nuclei (blue). Scale bars: 10 μm. We could clearly see LECs formed more focal adhesion kinase on viscoelastic hydrogel (A) compared to the elastic hydrogel (D). Moreover, LECs showed more organized F-actin structure on viscoelastic hydrogel (E).

NMR spectra

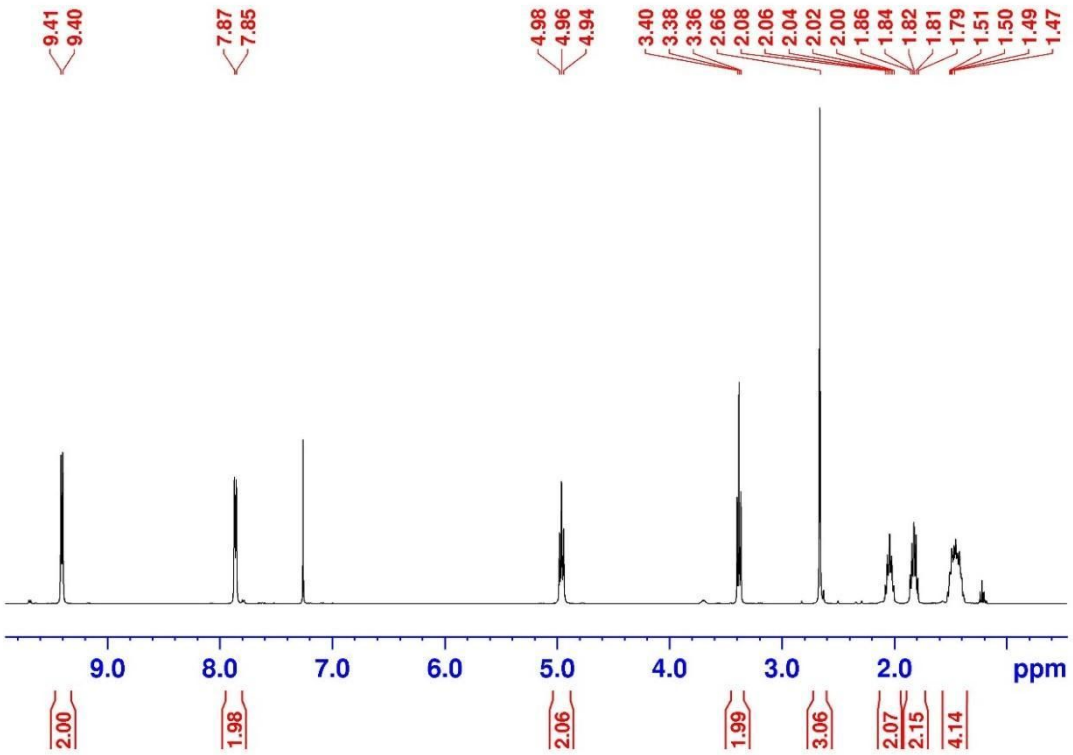

Figure S17. [1]H NMR spectrum of compound **1**.

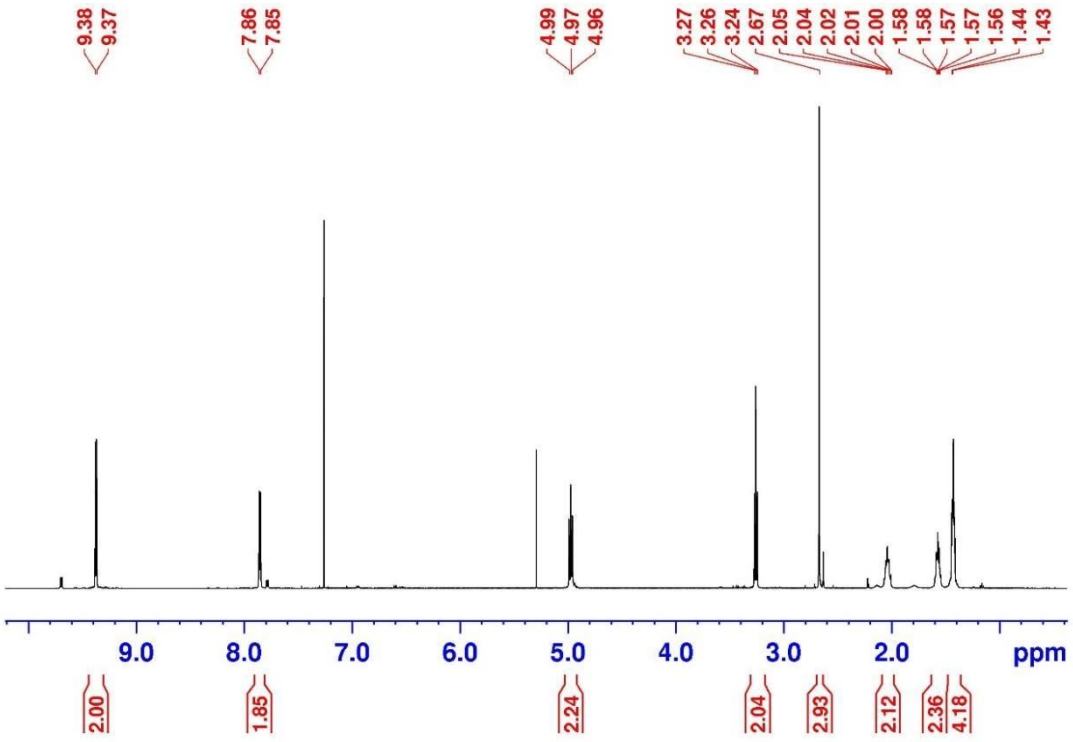

Figure S18. [1]H NMR spectrum of compound **2**.

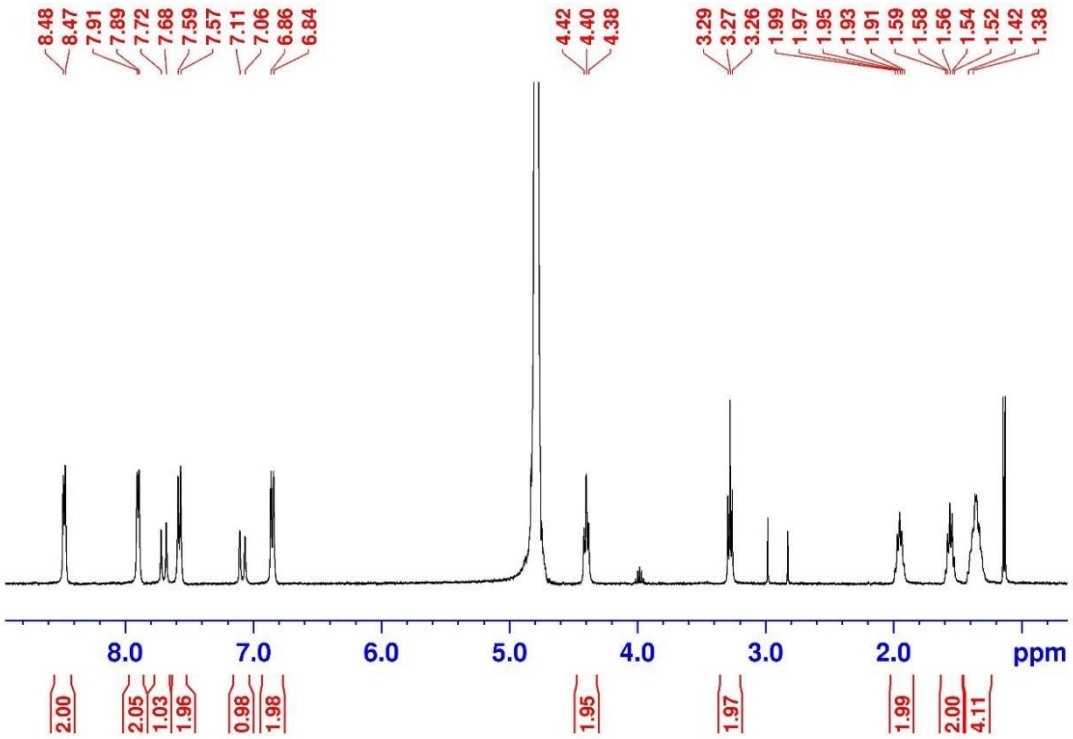

Figure S19. [1]H NMR spectrum of compound **BM-azide**.

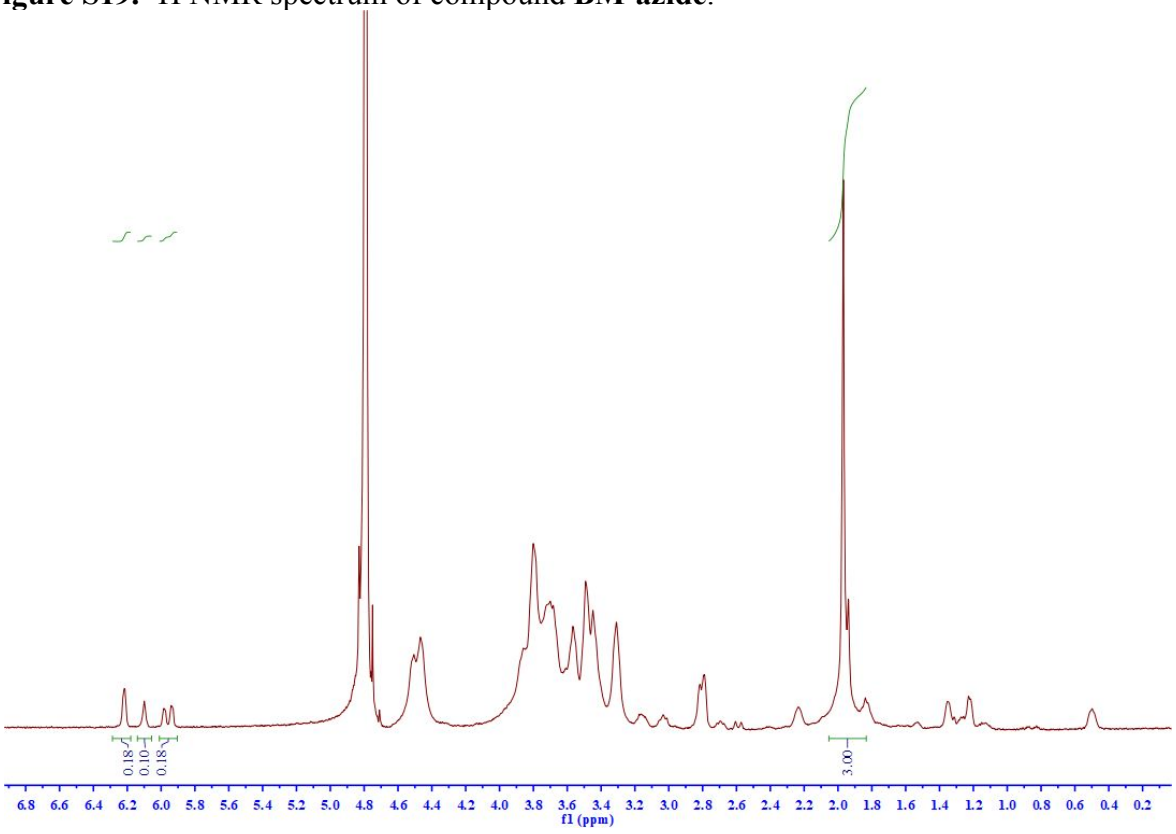

Figure S20. [1]H NMR spectrum of HA-Nor with DS value 23%.

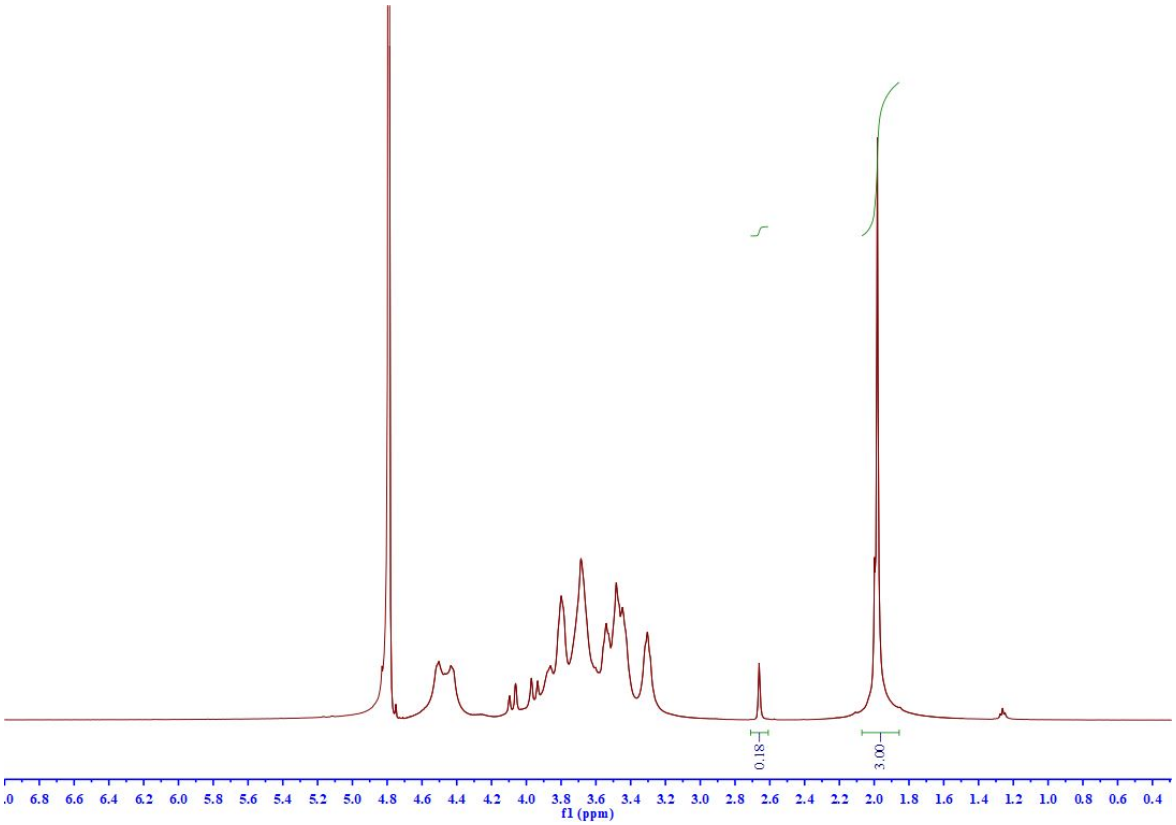

Figure S21. [1]H NMR spectrum of HA-alkyne with DS value 18%.

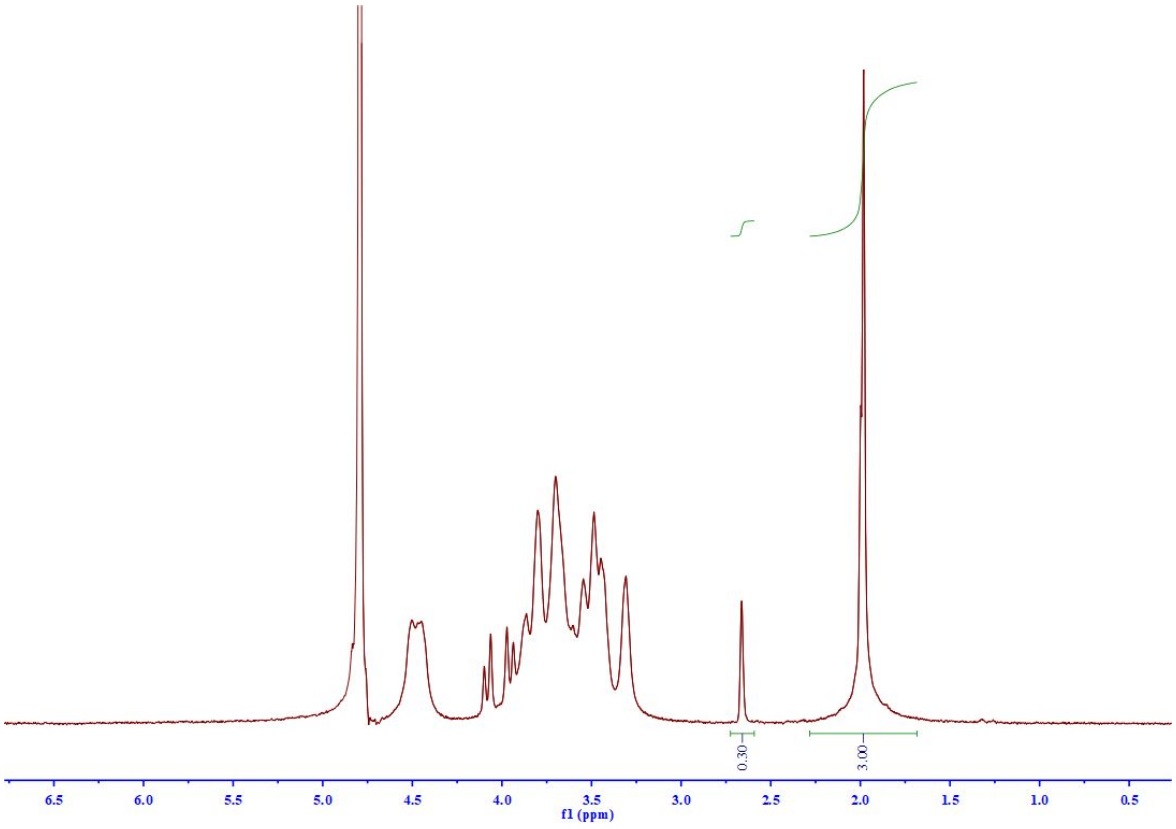

Figure S22. [1]H NMR spectrum of HA-alkyne with DS value 30%.

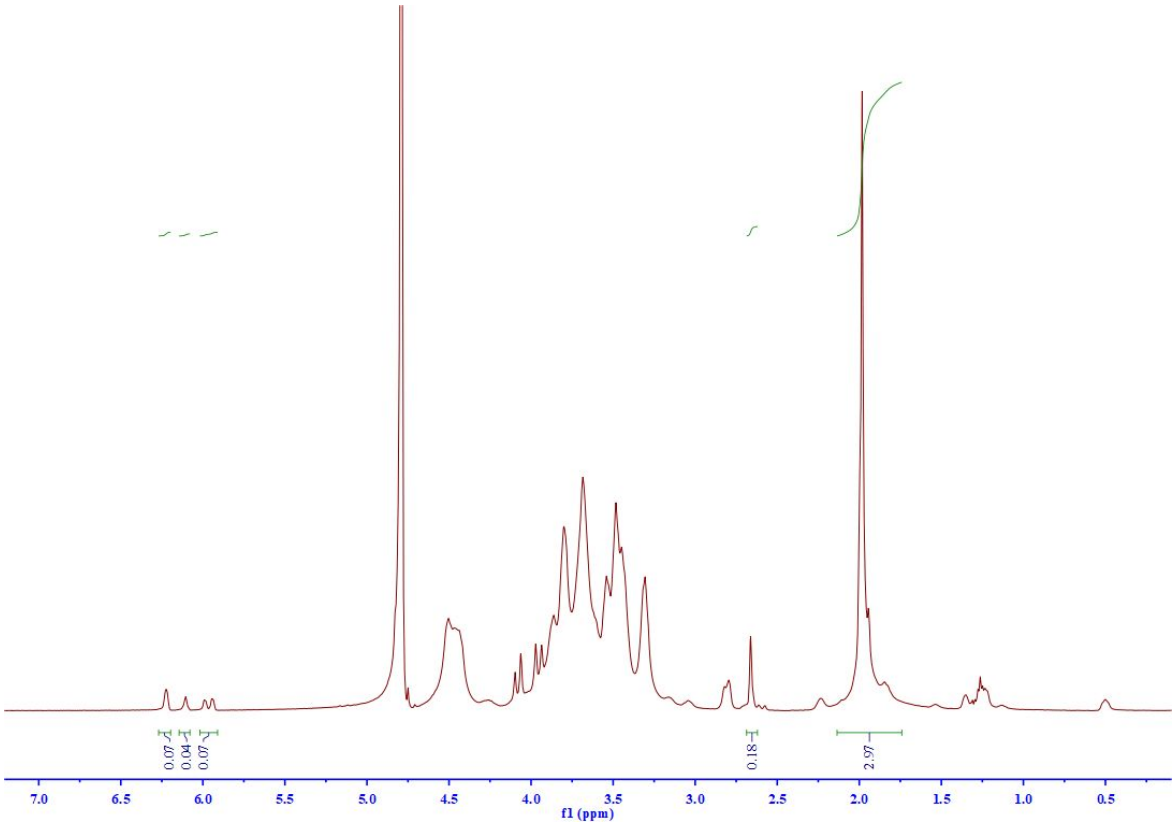

Figure S23. [1]H NMR spectrum of HA-Nor/alkyne with DS value 8% for Nor and 18% for alkyne.

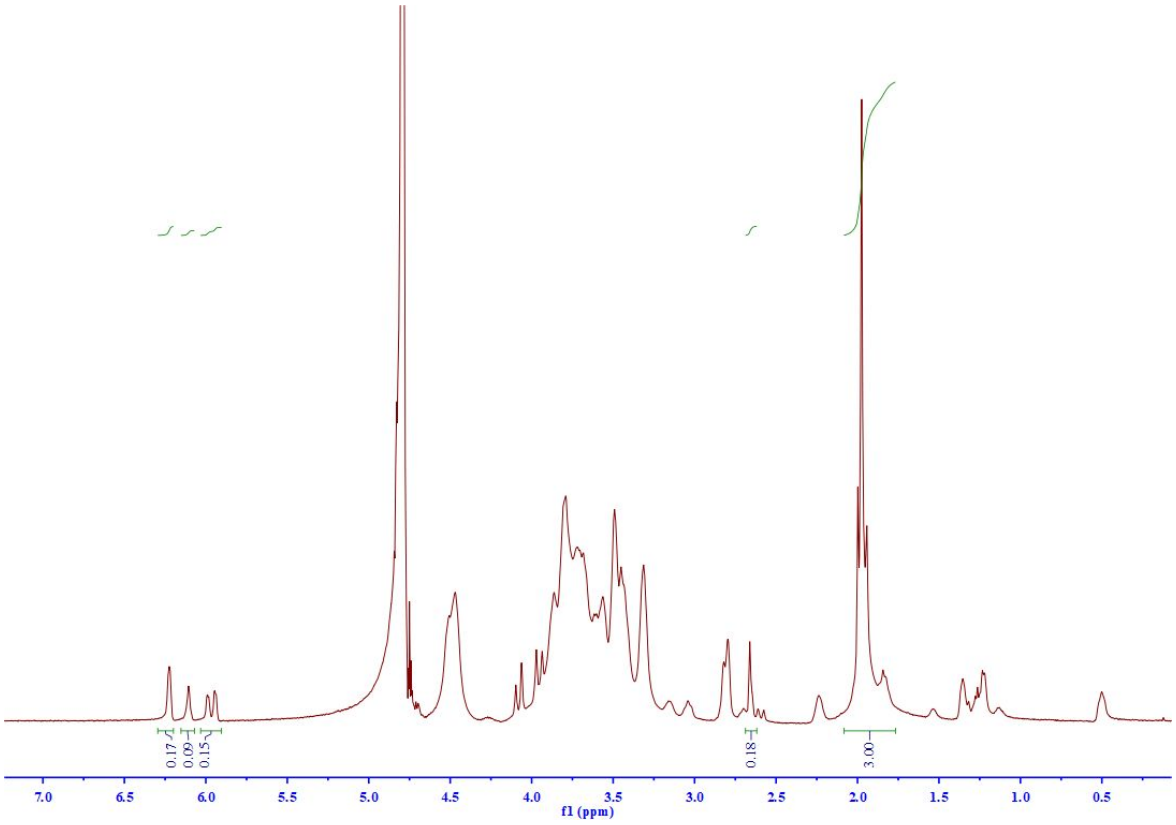

Figure S24. [1]H NMR spectrum of HA-Nor/alkyne with DS value 20% for Nor and 18% for alkyne.

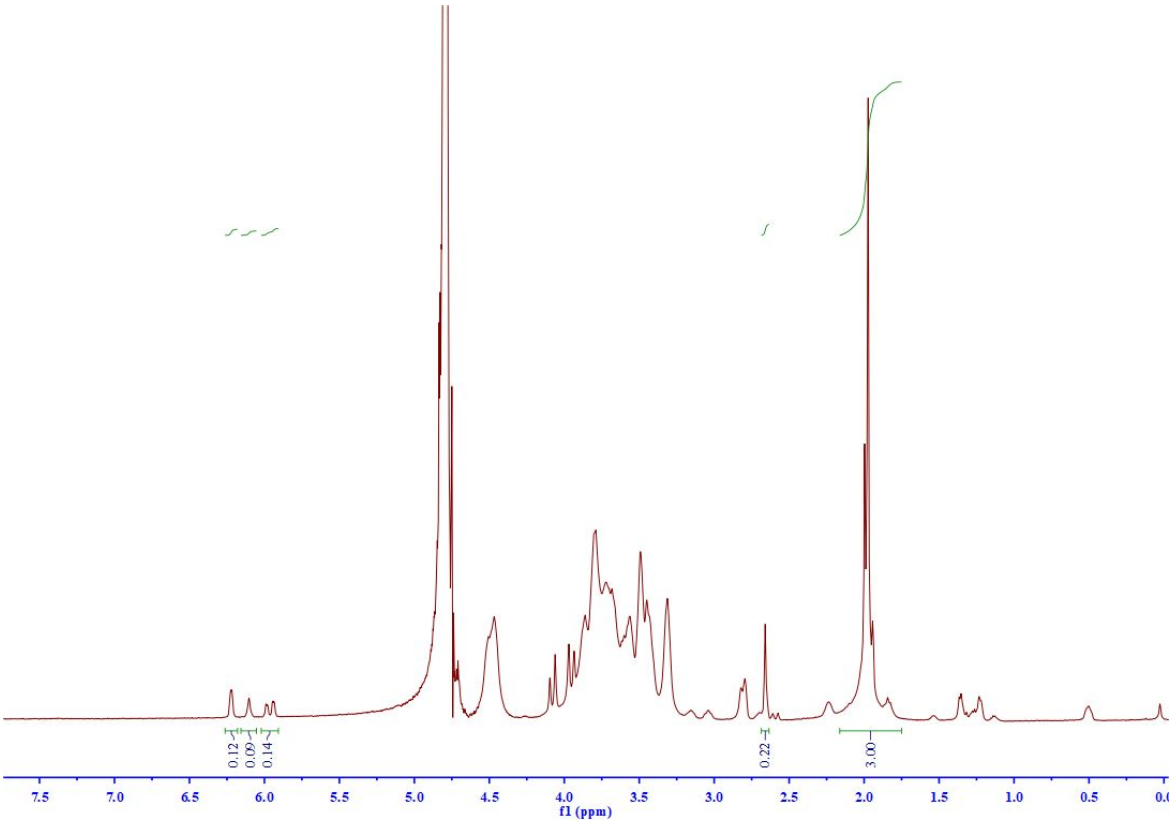

Figure S25. ^{1}H NMR spectrum of HA-Nor/alkyne with DS value 18% for Nor and 22% for alkyne.

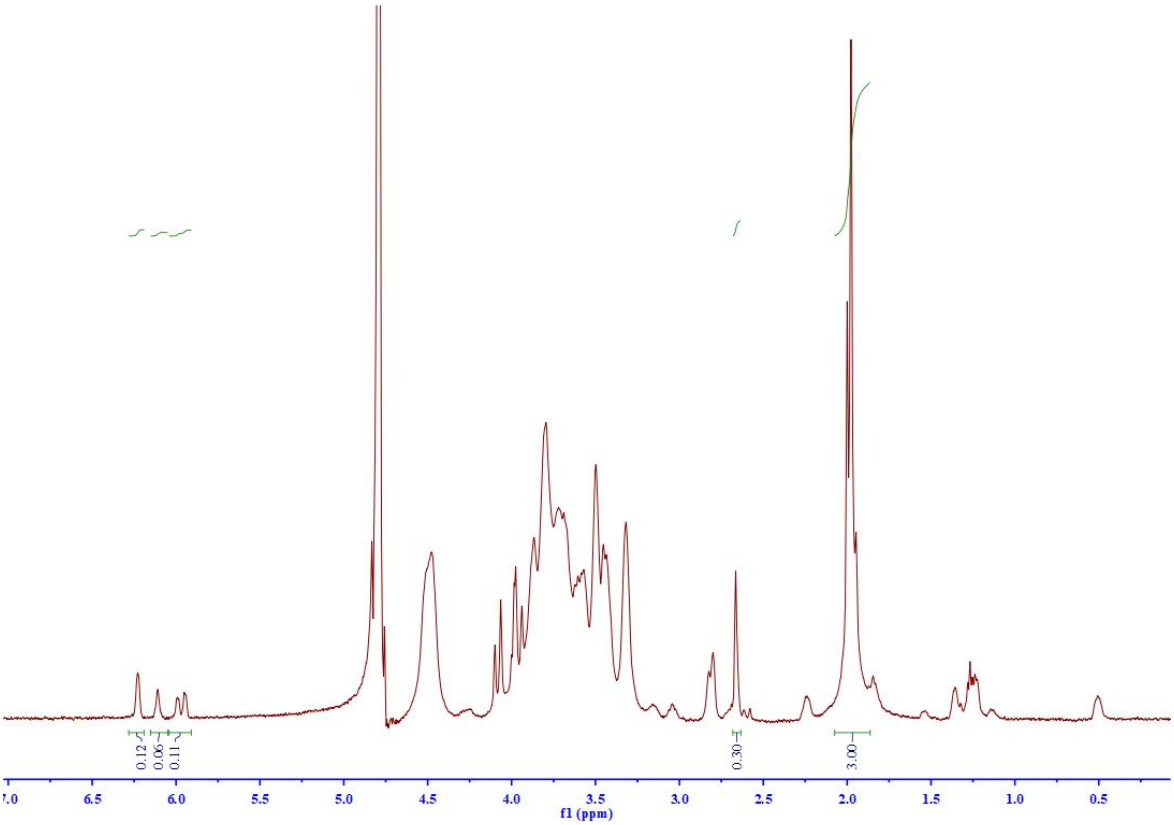

Figure S26. ^{1}H NMR spectrum of HA-Nor/alkyne with DS value 15% for Nor and 30% for alkyne.

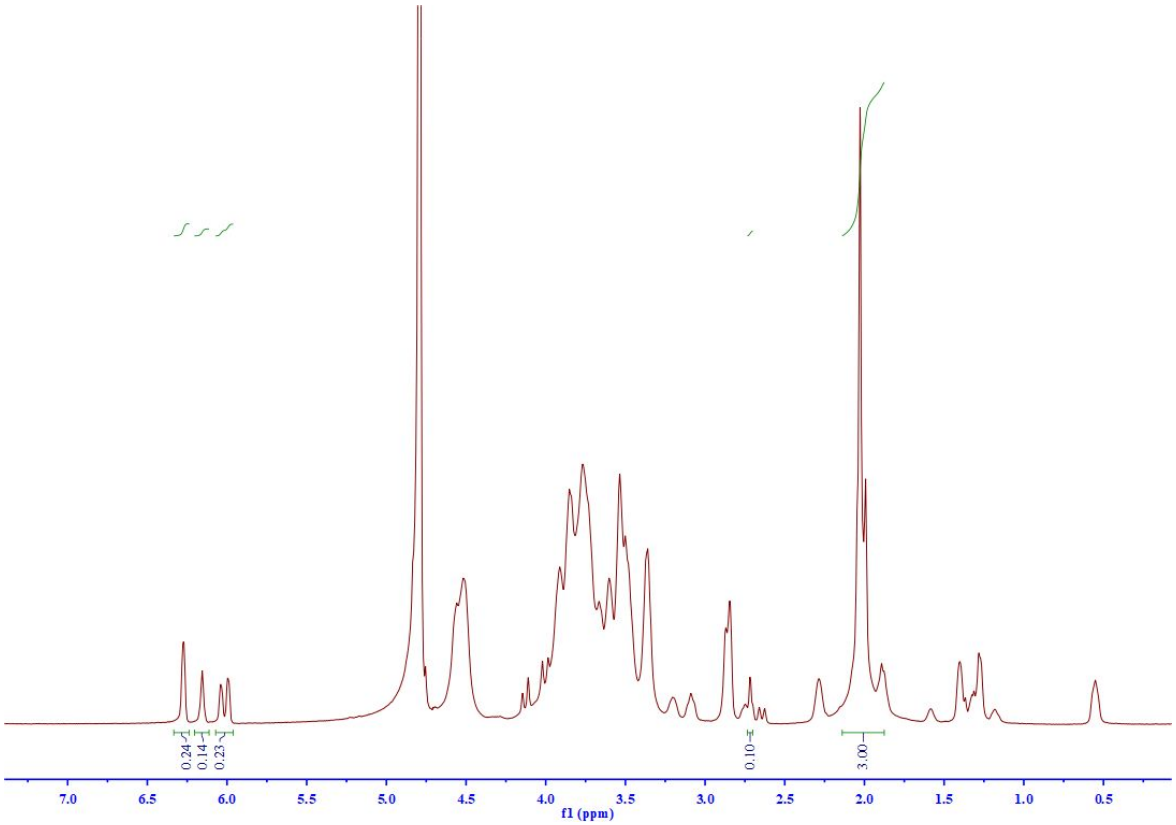

Figure S27. [1]H NMR spectrum of HA-Nor/alkyne with DS value 30% for Nor and 10% for alkyne.

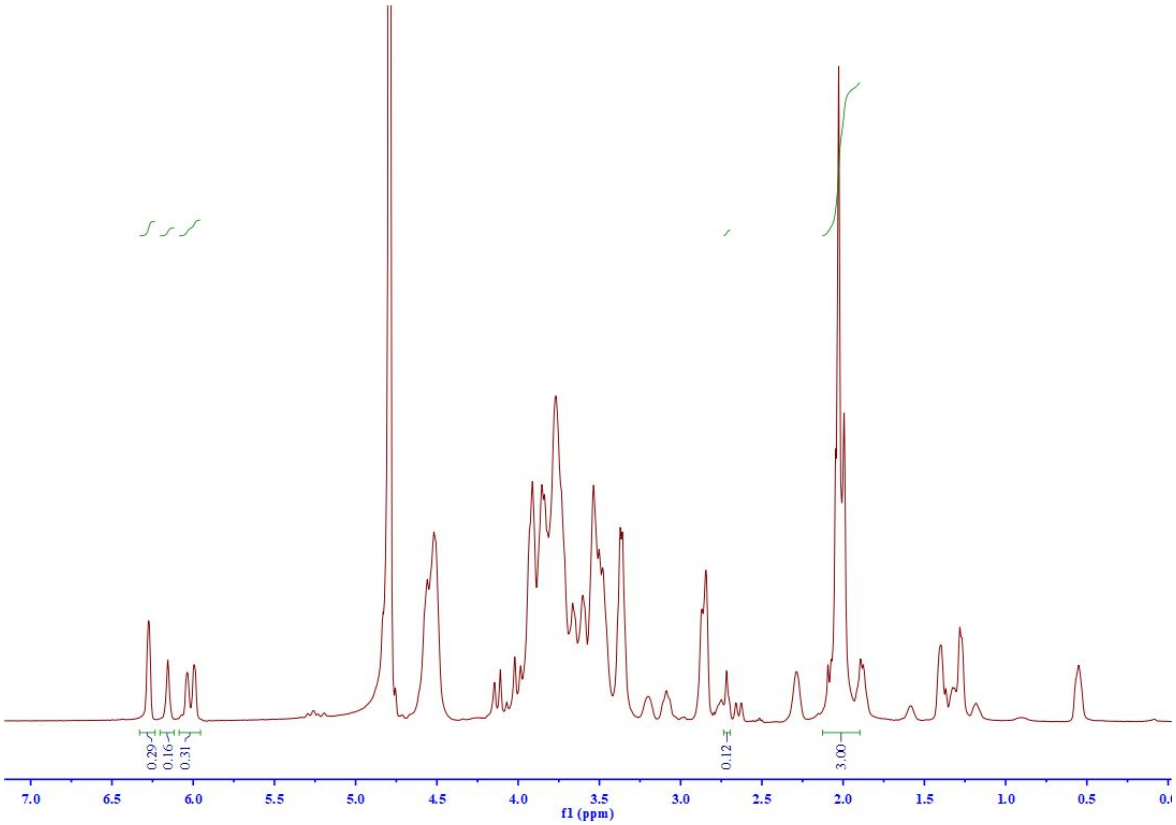

Figure S28. [1]H NMR spectrum of HA-Nor/alkyne with DS value 38% for Nor and 12% for alkyne.

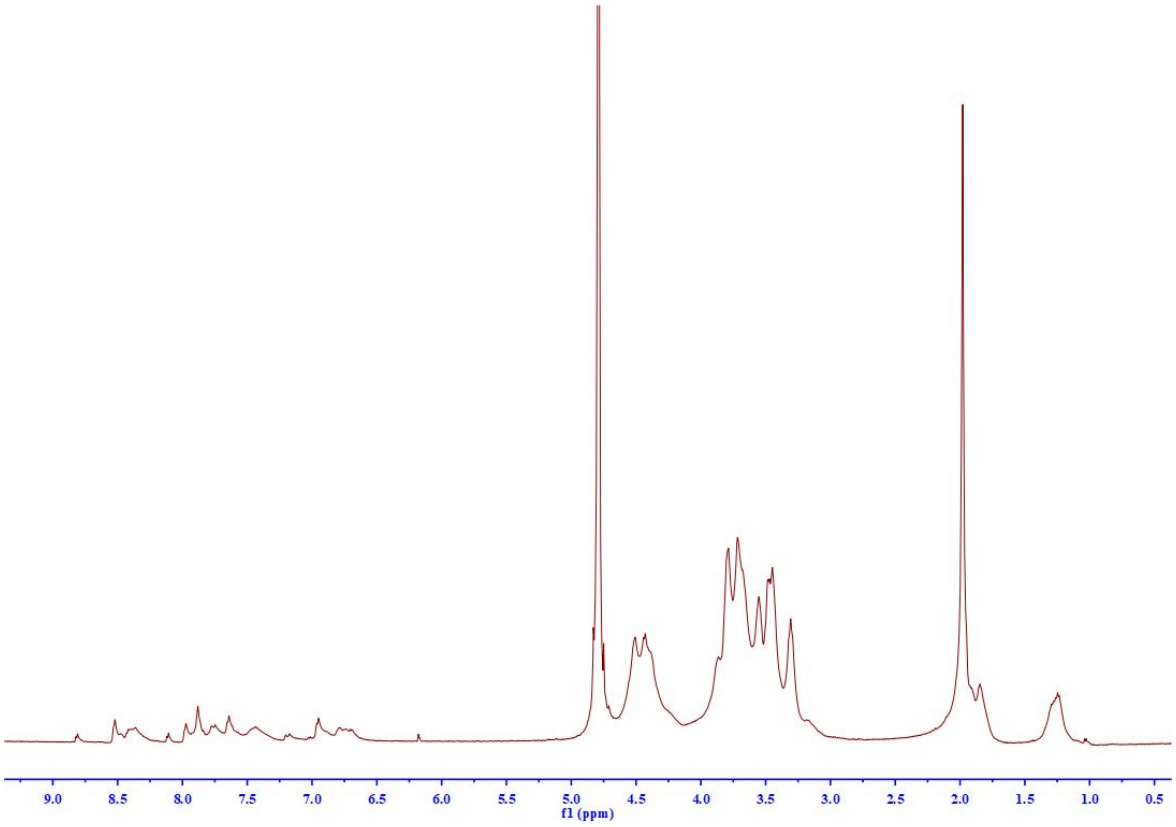

Figure S29. ^{1}H NMR spectrum of HA-BM with DS value 18%.

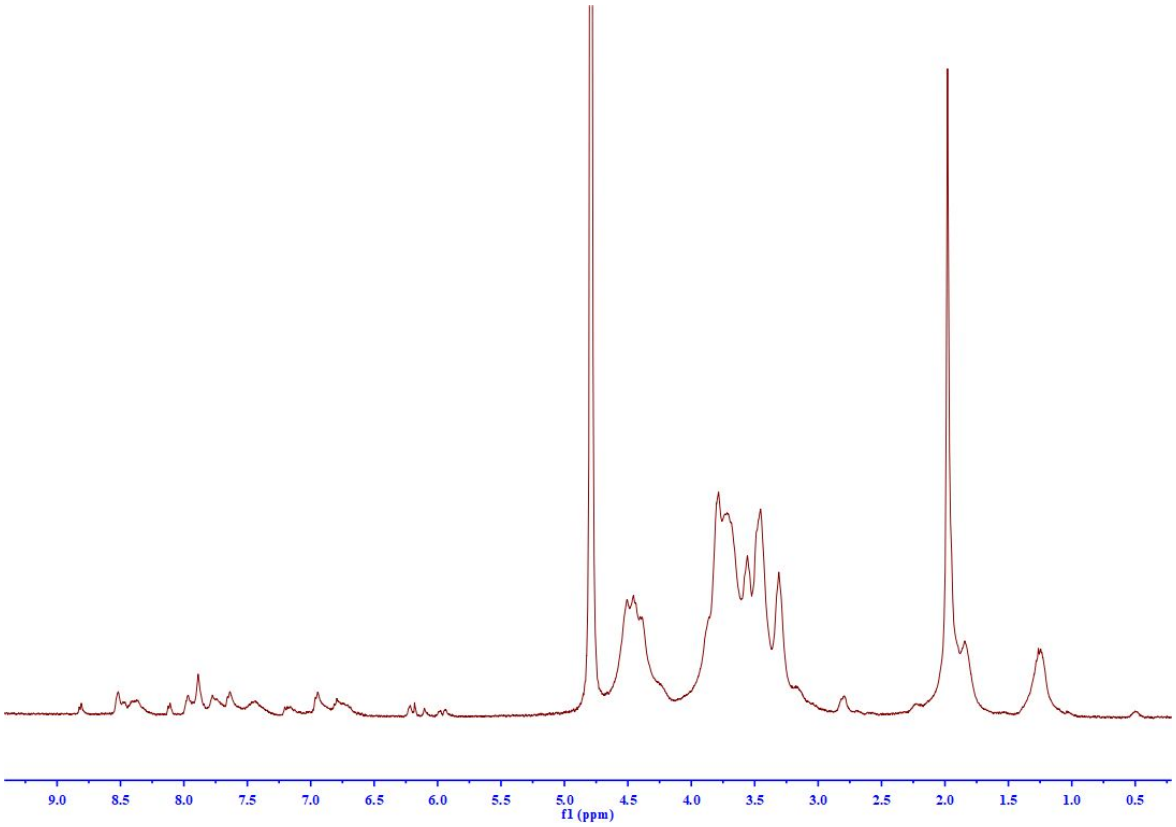

Figure S30. ^{1}H NMR spectrum of HA-Nor/BM with DS value 8% for Nor and 18% for BM.

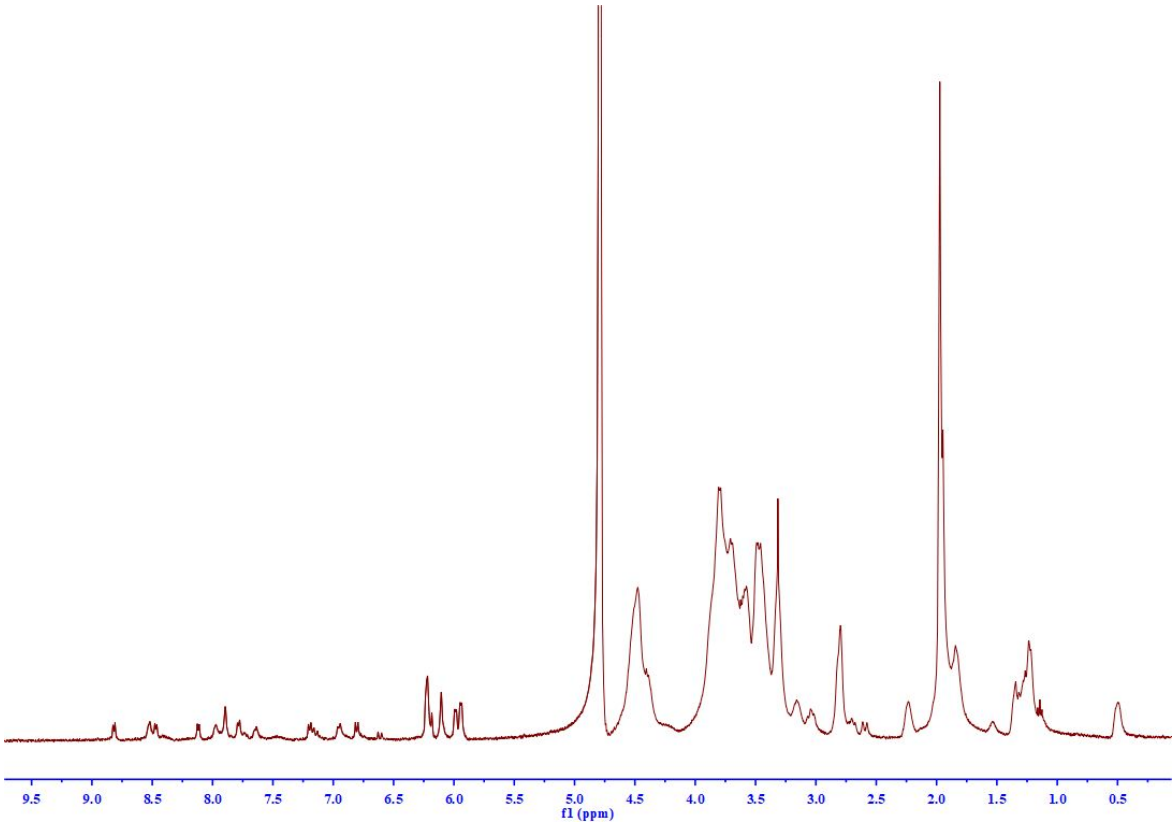

Figure S31. ^{1}H NMR spectrum of HA-Nor/BM with DS value 30% for Nor and 10% for BM.